Supplement A: Andean Slip Layer Viscosity (SLV) derived from quasi-steady equilibrium between tectonic and buoyancy forces

Supplementary material for:

On the role of lithosphere-scale structures in the long-term seismotectonic segmentation of active margins: a case study in the Andes.

Gonzalo Yanez C.[1], Jose Piquer R.[2], Orlando Rivera H.[3]

(1): Pontificia Universidad Católica de Chile, Av. Vicuña Mackenna 4860, Macl, Santiago, Chile, gyanez@ing.puc.cl

(2): Instituto de Ciencias de la Tierra, Universidad Austral de Chile, jose.piquer@uach.cl

(3): Minera Peñoles de Chile, orlando_rivera@penoles.com.mx

Negative free air anomaly along the Chile-Peru Trench is the response to dynamic equilibrium between buoyancy and tectonic forces (Yañez and Cembrano, 2014) (Figure S.1). Tectonic force tends to drag the continental plate downwards, whereas buoyancy force restore this deformation (Figure s.1). At the equilibrium, the assumption of present-day configuration, the net force and long-term deformation (flow in continuum physics) should be zero. Therefore, given the observed bathymetry, the equilibrium is a function of the SLV.
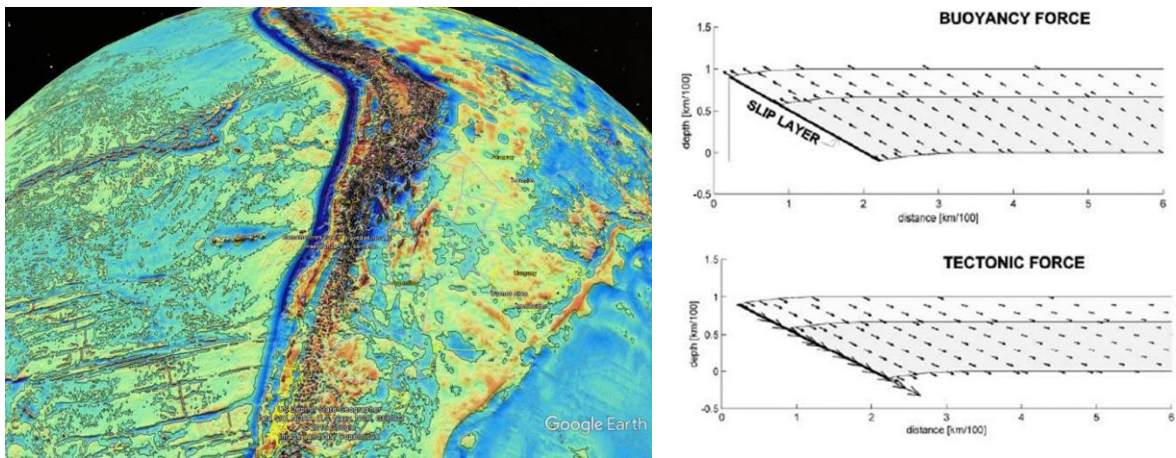
Figure S.1: Left panel, free air anomaly along the Andean region (EGM 2009, Sandwell et al., 2014). Negative anomaly in excess of -200 mGal at the trench represent the dynamic equilibrium of tectonic (convergence) and buoyancy forces (the deep-water column at the trench). Right panel, schematic representation of tectonic forces (lower right panel) that generates downward flow, and buoyancy forces (upper right panel) that force the flow in the opposite sense.

Following Yañez and Cembrano (2004) rational, we approximated the long-term force equation by Navier-Stokes partial differential equation for incompressible media:

$\mu\nabla^2\acute{u} - \nabla P = -\rho\hat{a}Gr$ (A1), in this equation:

- μ: viscosity, u: velocity, p: pressure, ρ: density, $\hat{a} = [\hat{x}, \hat{z}]$, Gr: Grashof number, $(Gr = g\rho_o x_o^2/\mu_o u_o)$, and g: gravitational acceleration (10 m/s^2)

The non-dimensional Grashof number represents the ratio between the buoyant and viscous (or tectonic) forces, r_o, x_o, μ_o, u_o, are the characteristic density (3300 kg/m3), length (100 km), viscosity (10^{22} Pa s); and plate velocity (6.6 cm/yr),respectively. We solve this problem using FLEXPDE 6.0 package for 2D finite element partial differential equations, using sparse lineal system solvers, with 363 triangular elements, and cubic element types. The problem uses the penalty formulation that replaces the pressure term for an incompressible fluid [i.e, Zienkiewicz and Taylor, 1991]. We use simple Newtonian rheology in order to keep the problem simple, but keeping the basic physics, which means characterizing the three main domains, crust, mantle, and slip layer. In Figure S.2, we present the boundary conditions and main finite elements domain for each traverse section.
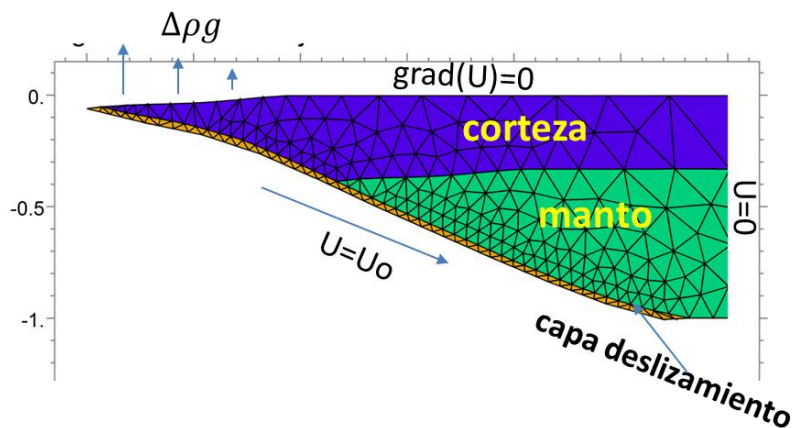
Figure S.2: Finite element section and boundary conditions.

We discretize the continental lithosphere in three domains, crust, mantle, and slip layer. Body forces operates against a reference model of an isostatic equilibrium crust of 33 km. Therefore, a thickened crust segment would exert an upward force. At the trench, the much lighter water column (density of 1,000 km/m3) exert an upward buoyancy force due to the lack of crustal material (density of 2700 km/m³). We balance these buoyancy forces with the tectonic forces expressed in terms of a velocity boundary condition at the Wadati-Benioff zone. We impose a zero velocity condition in the right hand side, at the cratonic area, characterized by null deformation. The remaining boundary conditions at the surface and lithosphere-asthenosphere boundary are null velocity gradients (Neumann boundary

condition). Relevant model parameters for crust and mantle are, density of 2700 Kg/m^3 and 3300 Kg/m^3, respectively, and the same effective viscosity of 10^{22} Pas for both domains. The geometry at each lithospheric section is determined through DTM (NOAA, 2022, DOI: 10.25921/fd45-gt74) for topography/bathymetry model and SLAB 2.0 (Hyes, 2018) for the shape of the Benioff-Wadatti plane. We compute the effective slip layer viscosity (SLV) by equating the tectonic and buoyancy forces at each transect. The general procedure involves the computation of a family of deformation models in the lithosphere for a range of SLV between 10^{19} to 10^{21} Pas. From these family models, the equilibrium effective viscosity is the one in which lithospheric deformation is minimum (see further details of this method in Yáñez and Cembrano (2004).The study area was discretized in sections parallel to the convergence direction every 20km (Figure S.3), completing 120 sections between 18°-44°S. Applying this approach, we obtain the equilibrium SLV at each section.
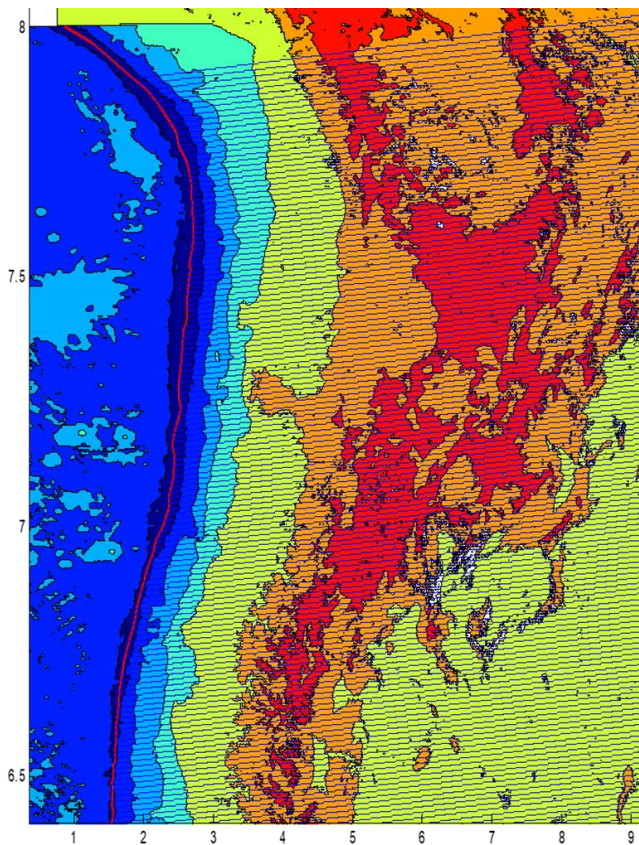
Figure S.3: Location of the lithospheric profiles (blue lines every 20km) used for the SLV modeling between Arica (18°S) and Chiloé (44°S). Underneath, the color map of the SRTM30 model.

II.1 Model results and separation of long and short-term components.

In Figure S.4a we present the results of the modeling in terms of the SLV of the 120 sections displayed in Figure S.3. The observed values ranges between 0.5-2.5 10^{20} Pas, with a clear trend of northward increment. This behavior was already observed in Yáñez and Cembrano (2004), and interpreted in terms of the age-thermal dependence of the effective viscosity at the slip layer zone. This northward increment in SLV implies a larger long-term plate coupling in the northern domain. This behavior successfully explain the observed high topography of northern Chile (Figure S.3) and the associated thicker crust assuming that crustal thickness is mostly related shortening. In fact, the exercise of generating present crustal thickness from a flat crust of 33 km, in a time window of 20 Ma (most of the Neogene, the likely period of Andean Uplift (Kley et al., 1999), and using the expected erosion rates (Carretier et al., 2013). In Yañez and Cembrano (2004), this regional coupling is associated to the increment in the subducting plate age northward. Although others authors (i.e. Lamb and Davies 2003), considers that the northward deficiency in sedimentary supply at the trench is the driving mechanism to explain the larger long term coupling in the Altiplano region. Although the discussion on the plate coupling main controlling factor(s) is still open, the northward increment in long term coupling is out of the question, and then for simplicity, we applied the empirical age (almost linear with respect to latitude) dependence established by Yañez and Cembrano (2004) to account for the regional plate coupling:

SLV_reg=10^{19}[0.031*(age**1.1)-0.137] [Pas]

In Figure S.4b this regional trend is presented along with the smooth SLV derived from the model effort. We prefer the smooth model in order to prevent bad computations of the equilibrium between tectonic and buoyancy forces in some exceptional cases where the geometry of the problem (topography/bathymetry, Benioff plane surface) present out of bound values. Looking at the regional trend of Figure S.4b we notice that effectively it represents an envelope of the computed SLV values, however is not

accounting for the whole signal. In fact amplitudes of 10-20% of the total, with wavelengths of 50-250 km remains unexplained by this model. Our working hypothesis is that this residual signal is associated with a short term plate coupling, as will be discussed in detail in next section. We proceed then to remove this regional trend, presenting the residual and normalized SLV (NRSLV) values in Figure S.4c.
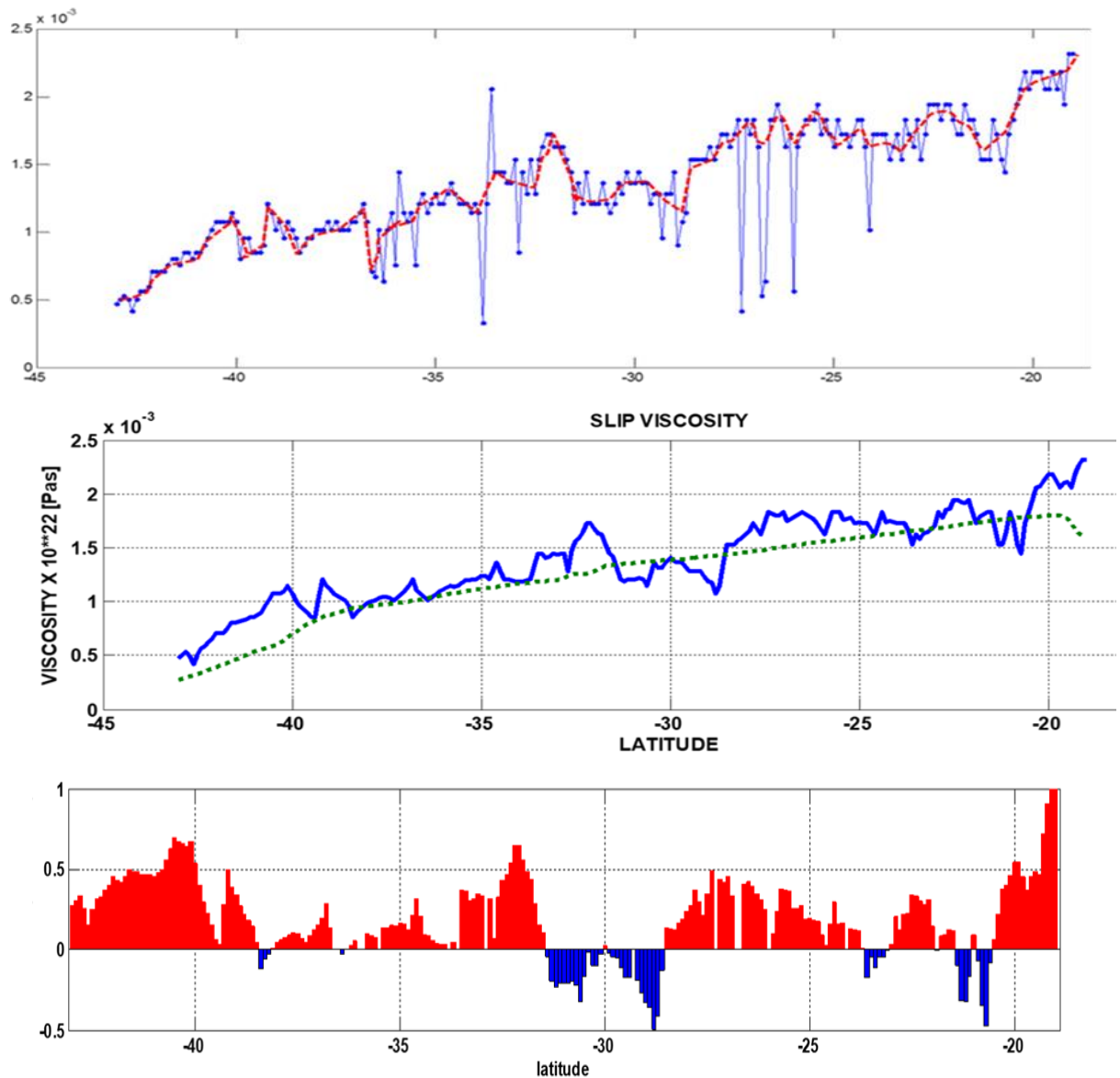
Figure S.4: (a) upper panel, SLV (x10^{23} Pas) (blue curve) against the latitude, red curve is a smooth version that accounts for the expected more continuous behavior along the plate coupling zone; (b) middle panel, smooth SLV (heavy blue) and regional trend from age dependence (Yañez and Cembrano, 2004) (segmented green); (c) lower panel, normalized residual SLV (NRSLV). The residual SLV is normalized by the maximum value observed at 18°S.

We use normalized values (NRSLV) in order to facilitate the discussion in the next section, given the semiquantitative argumentation available. At this regard, the exact meaning of positive and negative NRSLV values is not necessarily relevant, due to the fact that the regional trend removed is highly imprecise. But nevertheless, high/low values of NRSLV can be interpreted in our working hypothesis as high/low values of plate coupling. On the other hand, transitions between high and low values are probably a miss representation of a more complex reality, given the low pass filter applied and the somehow integrative model construction. Despite all these shortcomings of this approach, we will show in next section that the correlation with some key first order elements of the Andean convergence provide compelling grounds to support the working hypothesis of use it as a proxy for the seismic plate coupling of the margin.

References

Carretier, S., Regard, V., Vassallo, R., Aguilar, G., Martinod, J., Riquelme, R., ... & Lagane, C. (2013). Slope and climate variability control of erosion in the Andes of central Chile. Geology, 41(2), 195-198.

J. Kley, C.R. Monaldi, J.A. Salfity. (1999). Along-strike segmentation of the Andean foreland: causes and consequences, Tectonophysics,Volume 301, Issues 1–2, Pages 75-94, ISSN 0040-1951, https://doi.org/10.1016/S0040-1951(98)90223-2.

Lamb, S., & Davis, P. (2003). Cenozoic climate change as a possible cause for the rise of the Andes. Nature, 425(6960), 792-797.

Sandwell, D. T., Müller, R. D., Smith, W. H., Garcia, E., & Francis, R. (2014). New global marine gravity model from CryoSat-2 and Jason-1 reveals buried tectonic structure. Science, 346(6205), 65-67.

Yañez G., J. Cembrano. (2004) The role of the viscous plate coupling in the late tertiary Andean deformation. Journal of Geophysical Research, vol 106, 6325-6345, 2004.

Zienkiewicz, O. C., and R. L. Taylor (1991), The Finite Element Method, vol. 2, Solid and Fluid Mechanics Dynamics and Non-linearity, 4th ed., McGraw-Hill, New York.